Ecotoxicology and Environmental Safety 205 (2020) 111186

Contents lists available at ScienceDirect

Ecotoxicology and Environmental Safety

journal homepage: www.elsevier.com/locate/ecoenv

NADPH oxidase and mitochondria are relevant sources of superoxide anion in the oxinflammatory response of macrophages exposed to airborne particulate matter

Lourdes Cáceres [a], Mariela L. Paz [c,d], Mariana Garcés [a], Valeria Calabró [a,b], Natalia D. Magnani [a,b], Manuela Martinefski [e], Pamela V. Martino Adami [f], Laura Caltana [g], Deborah Tasat [h], Laura Morelli [f], Valeria Tripodi [e], Giuseppe Valacchi [i,j], Silvia Alvarez [k,b], Daniel González Maglio [c,d], Timoteo Marchini [a,b], Pablo Evelson [a,b,*]

[a] Universidad de Buenos Aires, Facultad de Farmacia y Bioquímica, Departamento de Química Analítica y Fisicoquímica, Cátedra de Química General e Inorgánica, Argentina
[b] CONICET - Universidad de Buenos Aires, Instituto de Bioquímica y Medicina Molecular (IBIMOL), Facultad de Farmacia y Bioquímica, Argentina
[c] Universidad de Buenos Aires, Facultad de Farmacia y Bioquímica, Departamento de Microbiología, Inmunología, Biotecnología y Genética, Cátedra de Inmunología, Argentina
[d] CONICET - Universidad de Buenos Aires, Instituto de Estudios de la Inmunidad Humoral (IDEHU), Facultad de Farmacia y Bioquímica, Argentina
[e] Universidad de Buenos Aires, Facultad de Farmacia y Bioquímica, Departamento de Tecnología Farmacéutica, Cátedra de Tecnología Farmacéutica I, Argentina
[f] Laboratory of Brain Aging and Neurodegeneration, Fundación Instituto Leloir, IIBBA-CONICET, Argentina
[g] CONICET - Universidad de Buenos Aires, Instituto de Biología Celular y Neurociencia Prof. E. De Robertis (IBCN), Facultad de Medicina, Argentina
[h] Universidad Nacional de San Martín, Escuela de Ciencia y Tecnología, Centro de Estudios en Salud y Medio Ambiente, Argentina
[i] NC State University, Plants for Human Health Institute, Animal Science Department, USA
[j] Department of Life Sciences and Biotechnology, University of Ferrara, Ferrara, Italy
[k] Universidad de Buenos Aires, Facultad de Farmacia y Bioquímica, Departamento de Química Analítica y Fisicoquímica, Cátedra de Fisicoquímica, Argentina

ARTICLE INFO

Keywords:
Air pollution
Oxidative stress
Inflammation
Mitochondria
NADPH oxidase
Macrophages

ABSTRACT

Exposure to ambient air particulate matter (PM) is associated with increased cardiorespiratory morbidity and mortality. In this context, alveolar macrophages exhibit proinflammatory and oxidative responses as a result of the clearance of particles, thus contributing to lung injury. However, the mechanisms linking these pathways are not completely clarified. Therefore, the oxinflammation phenomenon was studied in RAW 264.7 macrophages exposed to Residual Oil Fly Ash (ROFA), a PM surrogate rich in transition metals. While cell viability was not compromised under the experimental conditions, a proinflammatory phenotype was observed in cells incubated with ROFA 100 μg/mL, characterized by increased levels of TNF-α and NO production, together with PM uptake. This inflammatory response seems to precede alterations in redox metabolism, characterized by augmented levels of H_2O_2, diminished GSH/GSSG ratio, and increased SOD activity. This scenario resulted in increased oxidative damage to phospholipids. Moreover, alterations in mitochondrial respiration were observed following ROFA incubation, such as diminished coupling efficiency and spare respiratory capacity, together with augmented proton leak. These findings were accompanied by a decrease in mitochondrial membrane potential. Finally, NADPH oxidase (NOX) and mitochondria were identified as the main sources of superoxide anion ($O_2^{\bullet-}$) in our model. These results indicate that PM exposure induces direct activation of macrophages, leading to

Abbreviations: ATP, Adenosine Triphosphate; AU, Arbitrary Units; CD80, Cluster of Differentiation 80; DAF-FM, 4-amino-5-methylamino-2′,7′-difluorofluorescein; DCF, 2′, 7′-dichlorofluorescein; DMEM, Dulbecco's Modified Eagle Medium; EDS, Energy Dispersive X-ray Spectroscopy; FCCP, Carbonylcyanide-4 (trifluoromethoxy)phenylhydrazone; GSH, Reduced glutathione; GSSG, Oxidized glutathione; MFI, Mean Fluorescence Intensity; MHC, Major Histocompatibility Complex; NOX, NADPH oxidase; Nrf2, Nuclear factor erythroid 2-related factor 2; OCR, Oxygen consumption rate; PM, Particulate matter; ROFA, Residual Oil Fly Ash; ROS, Reactive Oxygen Species; SOD, Superoxide dismutase; TBARS, Thiobarbituric Acid Reactive Substances; TLR, Toll-like receptor; TMRM, Tetramethylrhodamine Methyl Ester; TNF-α, Tumor Necrosis Factor-α.

* Corresponding author. Universidad de Buenos Aires, Instituto de Bioquímica y Medicina Molecular (IBIMOL UBA-CONICET), Facultad de Farmacia y Bioquímica, Junín 954, C1113AD, Buenos Aires, Argentina.
E-mail address: pevelson@ffyb.uba.ar (P. Evelson).

https://doi.org/10.1016/j.ecoenv.2020.111186
Received 6 May 2020; Received in revised form 8 August 2020; Accepted 14 August 2020
Available online 24 August 2020

inflammation and increased reactive oxygen species production through NOX and mitochondria, which impairs antioxidant defense and may cause mitochondrial dysfunction.

1. Introduction

In their last report, the World Health Organization (WHO) estimates that 7 million premature deaths occur every year due to air pollution exposure, that are mainly attributable to stroke, ischemic heart disease, chronic obstructive pulmonary disease, and lung cancer (WHO, 2018).

Besides the well demonstrated toxicity of air pollution gaseous components, such as NOx, SO_2, O_3, and CO, epidemiological studies indicate that particulate matter (PM) is the main responsible for pollution exposure adverse effects (Brook et al., 2010). PM derived from anthropogenic emissions is a complex mixture of particles of variable sizes and chemical composition. Motor vehicle emissions and fossil fuel combustion during industrial processes and power generation are the main sources of PM in urban areas, as a result from incomplete oxidation of carbonaceous materials. In this context, Residual Oil Fly Ash (ROFA) is a PM surrogate comprised of particles with an aerodynamic diameter $\leq$ 2.5 μm ($PM_{2.5}$), rich in soluble transition metals (such as iron, vanadium, and nickel) Chen et al., 2004capable of initiating Fenton-like chemical reactions and oxidative damage. Taking into consideration ROFA's high content in metal ions, it is frequently used to study oxidative stress and inflammation following PM exposure.

Previously published reports have shown that PM exposure induces lung injury in humans (Chen and Lippmann, 2009Ghio and Devlin, 2001). Moreover, cigarette smoke enhances superoxide anion ($O_2^{\bullet-}$) production via NADPH oxidase (NOX) isoforms in the airway epithelium and mucosa (Loffredo et al., 2018a, 2018b; Moon et al., 2009). In accordance with these findings, pulmonary oxidative stress (Magnani et al., 2011; Prado et al., 2019) and inflammation (Marchini et al., 2014; Martin et al., 2019) have been reported in mice. Interestingly, as well as inflammatory leukocytes, lung epithelial cells, fibroblasts and dendritic cells incubated with ROFA have shown increased proinflammatory cytokines release *in vitro* (Arantes-Costa et al., 2014; Gao et al., 2004; Marchini et al., 2016; Orona et al., 2014), thus accounting for local inflammation in the lung following PM exposure. Moreover, systemic inflammation has also been reported in exposed mice (Marchini et al., 2014), and found to be involved in the development of impaired contractile function and cardiac remodeling following myocardial infarction, which was prevented by blocking circulating TNF-α (Marchini et al., 2015) and by alveolar macrophage depletion (Marchini et al., 2016). Current evidence suggests that alveolar macrophages play a central role in the mechanisms triggered by PM exposure (Tang et al., 2019) that might be associated with the reported oxinflammatory response (Valacchi et al., 2018). However, there is still debate on the sequence of events between inflammation and oxidative stress triggered after PM exposure (Sijan et al., 2015).

After an acute exposure to PM, the innate immune system is activated, where macrophages play a key role by releasing proinflammatory mediators, such as TNF-α, IL-6, and IL-1β (Miyata and van Eeden, 2011). In addition, macrophages can exacerbate $O_2^{\bullet-}$ release mainly through the activation of cytosolic NADPH oxidase isoform 2 (NOX2) (Kampfrath et al., 2011), which might induce mitochondrial dysfunction and oxidative stress (Liu et al., 2019; Zhao et al., 2016). It is well documented that mitochondria produce H_2O_2 and $O_2^{\bullet-}$, in respiratory complexes I and III as a result of the electron transfer chain, and that this production could be enhanced because of mitochondrial dysfunction (Brand, 2016). Also, recent research has pointed out mitochondria as orchestrators of the immune response by modulating metabolic and physiologic responses in macrophages (Breda et al., 2019), which could be the case in PM exposed cells.

Therefore, the aim of our work is to characterize the macrophage cell line RAW 264.7 response after an acute exposure to ROFA in terms of inflammation and oxidative metabolism, unravelling the mechanism linking both pathways.

2. Materials and methods

2.1. Drugs and chemicals

All chemicals were purchased from Sigma-Aldrich Chemical Company (St. Louis, MO, US), and cell culture reagents were provided by Gibco (Thermo Fisher Scientific, Waltham, MA, US) except for fetal bovine serum, which was purchased from Internegocios S.A. (Mercedes, BA, Argentina). The fluorescent probes 2′,7′-dichlorofluorescein (DCF) diacetate, 4-amino-5-methylamino-2′,7′-difluorofluorescein (DAF-FM) diacetate, AmplexRed, MitoSOX, and tetramethylrhodamine methyl ester (TMRM) were purchased from Invitrogen (Eugene, OR, US). ELISA detection kits were provided by BD Biosciences (San Jose, CA, US), and protease inhibitor cocktail set III was purchased from Calbiochem (San Diego, CA, US). MHC type II and CD80 antibodies were provided by eBioscience (San Diego, CA, US).

2.2. Cell culture

Murine macrophage cell line RAW 264.7 was cultured in Dulbecco's modified Eagle medium (DMEM) supplemented with 10% fetal bovine serum, 100 U/mL penicillin, 100 μg/mL streptomycin, and 0.29 mg/mL L-glutamine. Cells were grown in plastic flasks in a 5% CO_2 humidified atmosphere at 37 °C, and medium was changed every 2–3 days until subconfluence was achieved. Then, cells were harvested using an EDTA 0.05% solution and placed thereafter in 6-well, 12-well or 24-well plates to perform all assays.

2.3. PM sample preparation

ROFA particles were collected from Boston Edison Co., Mystic Power Plant (Mystic, CT, US) burning low-sulfur residual oil (No. 6 fuel oil) and were kindly provided by Dr. J. Godleski (Harvard School of Public Health, MA, US). ROFA samples from this source have been characterized in terms of morphology and particle size by scanning electron microscopy using a Zeiss EVO 40 microscope (Carl Zeiss, Oberkochen, Germany). Elemental composition was assessed by energy dispersive X ray spectroscopy (EDS), revealing that vanadium, nickel and iron are the predominant metals present as water-soluble sulfates. Data analysis was carried out using INCA software (Oxford Instruments, Abingdon, Oxfordshire, United Kingdom) (Supplementary Fig. 1). ROFA suspension was prepared in DMEM followed by a 10-min ultrasonic water bath incubation before use. In addition, previously characterized Concentrated Ambient Particles (CAPs) (Magnani et al., 2015) were also tested to provide further evidence on the role of PM chemical composition.

2.4. RAW 264.7 incubation with ROFA

RAW 264.7 cells were incubated with 25, 50, or 100 μg/mL ROFA suspension to evaluate the effects of different PM concentrations, or DMEM as control condition for 24 h. Cell viability was assessed after 24 h incubation with ROFA with alamarBlue Cell Viability Reagent (Invitrogen), according to the manufacturer's instructions. Furthermore, in order to establish a time course for the response of such cells to PM, they were incubated with 100 μg/mL ROFA suspension or DMEM for 1, 3, 6, or 24 h and harvested afterwards. For reduced (GSH) and oxidized (GSSG) glutathione levels, thiobarbituric acid reactive substances (TBARS) and superoxide dismutase (SOD) activity assays, a cell lysate

was obtained after a 10-min incubation with cell lysis buffer (137 mM NaCl, 20 mM Tris-HCl, 2 mM EDTA, 10% glycerol, 1% Triton X-100, pH 8.00).

2.5. Cytokine quantification

TNF-α levels were quantified in cell culture supernatants using non-competitive ELISAs, according to the manufacturer's instructions. Results were expressed as pg/mL.

2.6. Intracellular redox status and NO production

The fluorescent probe DCF diacetate was used to evaluate the general intracellular oxidative status of RAW 264.7 cells incubated with ROFA at different concentrations and time points. In addition, DAF-FM diacetate served the purpose of NO detection. Cells were loaded with 5 μM DCF diacetate or 10 μM DAF-FM diacetate for 30 min at room temperature in the dark following a 20000-event acquisition in a FACSCalibur (BD Biosciences) equipment. Data were analyzed in the FL-1 channel with FlowJo software (Tree Star, Ashland, OR, US) (Marchini et al., 2014).

2.7. Cell surface markers

The expression of the cell surface markers MHC type II and CD80 was evaluated by flow cytometric analysis in RAW 264.7 cells after 24-h exposure to ROFA. Briefly, cells were harvested and stained with anti-MHC type II or anti CD80 fluorescence conjugated monoclonal antibodies for 30 min at 4 °C in the dark. Data acquisition and analysis were performed as previously described.

2.8. Reduced (GSH) and oxidized (GSSG) glutathione levels

The assessment of GSH and GSSG levels was performed by HPLC-MS/MS method as described by Lasagni Vitar et al. (2019) with slight modifications in the sample preparation. Briefly, cells cultured in 12 well plates were washed with MSTE buffer (0.23 M mannitol, 0.07 M sucrose, 10 mM Tris-HCl, 1 mM EDTA, pH 7.4) and 100 μL of cell lysing buffer were added to each well. The lysate was centrifuged at 800 g for 10 min at 4 °C. After centrifugation, a fraction of the supernatant was diluted $^1/_3$ with trifluoroacetic acid 10%-EDTA 1 mM, and the remaining sample was stored at −20 °C for protein content assessment by the Lowry assay (1951). Afterwards, the samples were centrifuged at 20, 000 g for 20 min at 4 °C and supernatants were separated. HPLC analysis was performed in a HPLC Ultimate 300 using a micro column BSD Hypersil C18 (100 × 2.1 mm d.i and 2.4 μm) and a mass detector TSQ Quantum Acess Max (Thermo Fisher Scientific). GSH and GSSG were eluted at a flow rate of 0.2 mL/min with methanol:ammonium formiate (1:99) (pH 3.5). Results were expressed as nmol/mg protein.

2.9. H_2O_2 steady state concentration

H_2O_2 steady state concentration was evaluated in cell culture supernatants by the Amplex Red-horseradish peroxidase (HRP) method (Chen et al., 2003). Resorfurin formation due to Amplex Red (25 μM) oxidation by HRP (0.5 U/mL) bound to H_2O_2 was measured in a PerkinElmer LS 55 Fluorescence Spectrometer (PerkinElmer, Waltham, US) at 563 nm (excitation) and 587 nm (emission). A calibration curve was performed using H_2O_2 as standard, and the results were expressed as μM concentration of H_2O_2.

2.10. Superoxide dismutase (SOD) assay

A colorimetric assay based on the inhibition of adrenochrome formation rate at 37 °C due to the addition of increasing amounts of cells lysate was performed. The reaction medium consisted in 1 mM epinephrine and 50 mM glycine buffer (pH 10.50). Measurements were performed at 480 nm in a Beckman DU 7400-diode array spectrophotometer (Beckman Coulter, CA, US). Enzymatic activity was expressed as the volume of sample needed to inhibit adrenochrome formation rate by 50% (USOD)/mg protein (Lasagni Vitar et al., 2015).

2.11. Phospholipid oxidation

Oxidative damage to phospholipids was evaluated as thiobarbituric acid reactive substances (TBARS) by a fluorometric assay. Briefly, 100 μL of cells lysate were mixed with 200 μL 0.1 N HCl, 30 μL 10% (w/v) phosphotungstic acid, 100 μL 0.7% (w/v) 2-thiobarbituric acid, and incubated at 95 °C for 60 min. Afterwards, samples were cooled and TBARS were extracted in 1 mL of n-butanol. After a 10-min centrifugation at 800*g*, the fluorescence of the butanolic layer was measured in a PerkinElmer LS 55 luminescence spectrometer (PerkinElmer) at 515 nm (excitation) and 553 nm (emission). A calibration curve was prepared using 1,1,3,3-tetramethoxypropane as standard (Casañas-Sánchez et al., 2016). Results were expressed as nmol TBARS/mg protein.

2.12. Transmission electron microscopy analysis

RAW 264.7 cells were cultured in 100 mm plates until subconfluence was achieved, and then incubated with DMEM or ROFA 100 μg/mL for 1 or 24 h. Samples were washed twice with PBS, following the sample preparation protocol described by Lasagni Vitar et al. (2015). Ultrathin sections were observed with a transmission electron microscope (TEM, Zeiss EM109; Carl Zeiss Meditec, Oberkochen, Germany), and representative digital images were captured using a charge-coupled device camera (ES1000W; Gatan, Inc., Pleasanton, CA, USA).

2.13. Cellular oxygen consumption rate (OCR) assays

RAW 264.7 cells were seeded at 16,000 cells per well in an XFp microplate (Seahorse Biosciences, North Billerica, MA, US) and incubated with DMEM or ROFA 100 μg/mL for 24 h, achieving an 80% confluence on the day of the assay. The assay was carried out as previously described by Adami et al. (2017). Briefly, an ATP synthase inhibitor (oligomycin, 2 μM), an uncoupler of oxidative phosphorylation (FCCP, 1 μM), and a mix of complex I and complex III inhibitors (rotenone and antimycin, final concentration 0.5 μM) were sequentially added throughout oxygen consumption rate (OCR) monitoring. Four baseline measurements and three response rates (after the addition of the different compounds) were measured, and the average of these rates used for data analysis. Respiratory parameters were obtained as follows: respiration driving proton leak: OCR after the addition of oligomycin; spare respiratory capacity: OCR after the addition of FCCP – baseline OCR; coupling efficiency: (baseline OCR - OCR after the addition of oligomycin)/baseline OCR.

2.14. Flow cytometry assessment of mitochondrial superoxide ($O_2^{\bullet-}$) production and mitochondrial membrane potential

RAW 264.7 cells were incubated with MitoSOX, a fluorescent probe targeted to live cells and sensitive to mitochondrial $O_2^{\bullet-}$ production, or TMRM, a cell-permanent dye that accumulates in active mitochondria with preserved membrane potential. Briefly, cells were loaded with 5 μM MitoSOX or 100 nM TMRM for 30 min at room temperature in the dark, following a 20,000-event acquisition in a FACSCalibur (BD Biosciences) equipment. Both MitoSOX and TMRM signals were analyzed in the FL-2 channel with FlowJo software (Tree Star) (Marchini et al., 2014).

2.15. NADPH oxidase (NOX) activity assay

The lucigenin-derived chemiluminescence method was used as an indirect measurement of NOX activity in the membrane fraction obtained from RAW 264.7 cells. Briefly, cells were washed twice with PBS

and scrapped in homogenization buffer (10 mM Tris-HCl pH 7.5, 1 mM EDTA, 1 mM EGTA) containing protease inhibitor cocktail set III (1:200). Samples were homogenized for 2 min with a motor pestle and centrifuged for 5 min at 500 g. Supernatants were recovered and centrifuged for 1 h at 100,000 g in a Beckman XL-90 ultracentrifuge (Beckman Coulter). The pellets were resuspended in 150 μL of homogenization buffer and passed through a syringe 20 times before use. Next, 150 μg of protein membranes were diluted in 250 μL of 50 mM phosphate buffer containing 1 mM EGTA and 150 mM sucrose (pH 7.4). Lucigenin (50 μM) was added to the reaction media, 100 μM NADPH was used as substrate, and chemiluminescence was continuously measured for 3 min in a Varioskan LUX microplate reader (Thermo Fisher Scientific). The specificity of the assay was confirmed by the addition of SOD (200 U/ml) as an $O_2^{\bullet-}$ scavenger. Results were expressed in arbitrary units (AU)/mg protein (Cervellati et al., 2015).

2.16. Statistics

Results were expressed as mean values ± standard error of the mean (SEM) of at least three independent experiments. Unpaired Student's t-test was used to analyze differences between two groups. ANOVA followed by Dunnett's Multiple Comparison Test was performed to analyze differences between more than two groups. Statistical significance was considered at $p < 0.05$.

3. Results

3.1. ROFA induces macrophage activation

PM cytotoxicity was evaluated in RAW 264.7 cells, at different ROFA concentrations (25, 50, and 100 μg/mL) after 24 h of incubation. No significant changes in cell viability were found within any experimental condition (Fig. 1a), which indicates that macrophages remain in an active metabolic state despite PM exposure.

In order to address inflammatory cell activation following PM incubation, TNF-α levels in cell culture supernatants were evaluated. Results showed a 20-fold increase in TNF-α levels ($p < 0.001$) in the ROFA 100 μg/mL experimental condition (Fig. 1b). Moreover, a 2-fold increase was found in NO production ($p < 0.001$), assessed as mean fluorescence intensity of the DAF-FM probe by flow cytometry (Fig. 1c and d), as opposed to the results obtained for Concentrated Ambient Particles (CAPs), a PM sample of different elemental composition (Supplementary Fig. 3). These results suggest a shift towards a classical proinflammatory phenotype of RAW 264.7 cells after ROFA, but not CAPs, incubation.

The expression of cellular surface markers, such as MHC class II and CD80, was also evaluated. Besides a slight decrease in CD80 at low concentrations of ROFA, no significant differences were observed in ROFA 100 μg/mL exposed cells (Supplementary Fig. 2). This result agrees with previous reports (Miyata and van Eeden, 2011), and may suggest that macrophages develop a nonspecific immune response in this model.

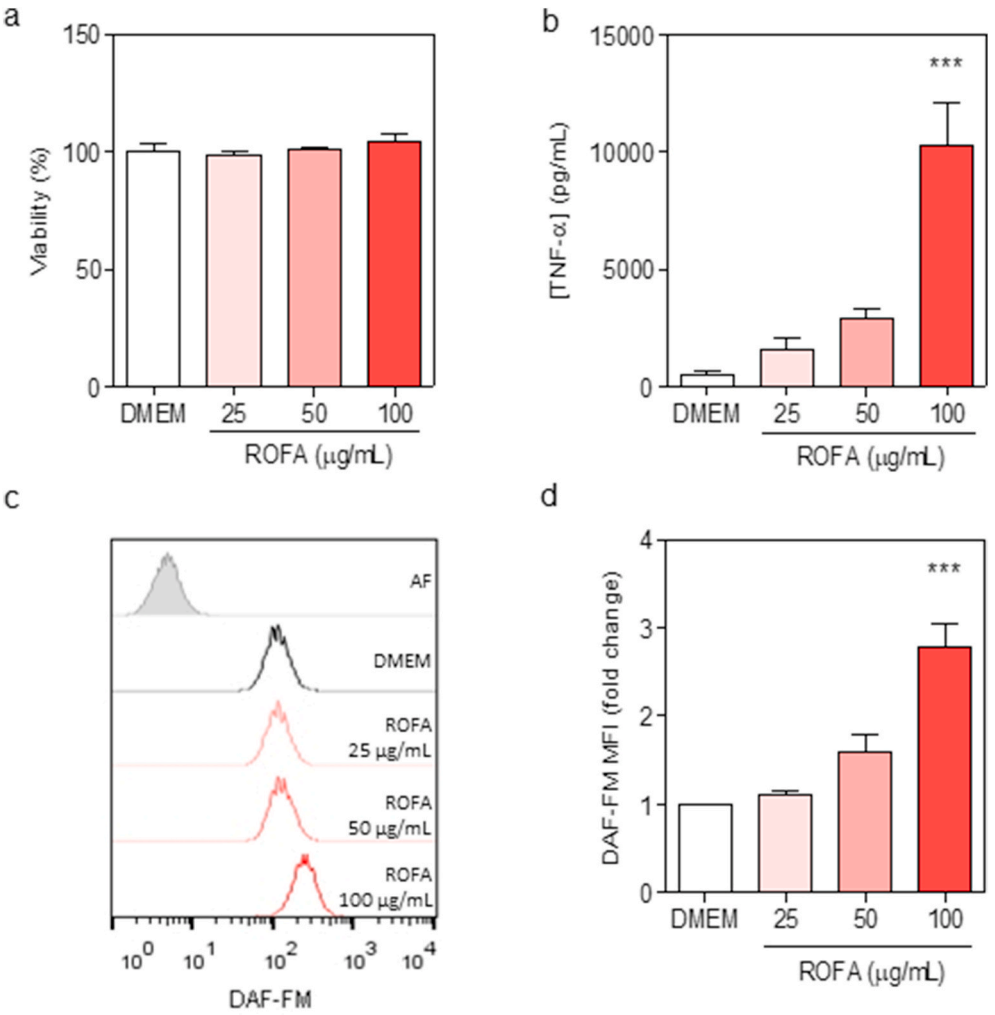

Fig. 1. Macrophage activation after ROFA incubation for 24 h. Cell viability was measured by the alamarBlue assay (a). TNF-α levels were quantified by ELISA in cell culture supernatants (b). NO levels were assessed by flow cytometric analysis of fluorescent signal from the DAF-FM probe, as shown by representative histograms and quantification of mean fluorescence intensity (MFI) as fold change relative to the DMEM group (c–d). Results are expressed as mean ± SEM of at least 3 independent experiments. ***$p < 0.001$, compared with DMEM group.

3.2. The oxidative status of macrophages is altered after ROFA exposure

There is a well-established relationship between inflammatory response and oxidative stress as a consequence of air pollution exposure (Ghio et al., 2002; Valacchi et al., 2016). In order to better characterize the oxidative status of ROFA-exposed macrophages, relevant indicators of the intracellular redox homeostasis were studied at different concentrations of PM. First, intracellular levels of oxidant species were assessed by flow cytometry as mean fluorescence intensity of DCF oxidation. A 2-fold increase ($p < 0.001$) in DCF signal was found in cells exposed to the highest ROFA concentration, when compared to the control group (Fig. 2a and b). Second, and since DCF oxidation is an indicator for nonspecific sources of oxidants, H_2O_2 steady state concentration was studied in cell culture supernatants by the AmplexRed fluorescent probe assay. Results showed a 2-fold increase for the 100 μg/mL ROFA-exposed cells (Fig. 2c).

Next, as glutathione is the major non-enzymatic intracellular antioxidant defense, GSH and GSSG levels were evaluated by HPLC-MS/MS. Although no significant alterations were found in GSH levels, the GSSG content increased up to 4-fold in RAW 264.7 cells incubated with ROFA 100 μg/mL ($p < 0.001$), which resulted in a decrease of the GSH/GSSG ratio (Fig. 2d) when compared to the control group. In addition, a 29% increase ($p < 0.05$) in SOD activity was observed in ROFA 100 μg/mL exposed macrophages (Fig. 2e). Finally, a 1-fold increase in TBARS content was found in ROFA 100 μg/mL exposed macrophages (Fig. 2f). Similar increments in DCF oxidation and TBARS content were obtained in RAW 264.7 cells exposed to CAPs (Supplementary Fig. 3). These data suggest that ROFA incubation induces alterations in oxidative status of macrophages, resulting in an inefficient antioxidant response, and increased levels of H_2O_2.

3.3. An inflammatory response precedes impaired redox metabolism in ROFA-exposed macrophages

In order to clarify the time course of the reported inflammatory response and oxidative imbalance, RAW 264.7 cell line was exposed to ROFA 100 μg/mL for 1, 3, 6 or 24 h. Results showed a 50-fold increase in TNF-α levels from cell culture supernatants ($p < 0.001$) and a 20% increase in NO production ($p < 0.001$) at 1 or 3 h after PM incubation, respectively (Fig. 3a and b). Within the evaluated experimental conditions, both TNF-α and NO levels reached their maximum at the 24-h time point. Interestingly, DCF oxidation augmented significantly only at the 24-h exposure time point (3-fold change, $p < 0.001$) (Fig. 3c).

Taking into consideration the results regarding macrophage activation, and to test whether it can be a consequence of direct particle uptake, the presence of ROFA particles inside the cell and morphological signs of cell activation were studied. When cytoplasmic complexity was assessed by flow cytometric analysis of light scattering properties (SSC-H), significant changes were observed in the distribution of the ROFA-exposed cell population (Fig. 4a and b). Moreover, transmission electron microscopy was carried out to confirm the presence of ROFA particles inside the cell (Fig. 4c). Preserved subcellular structures such as mitochondria in the control group (panels i and ii), and internalization of particles in the cytoplasmic space for both ROFA incubation time points (panels iii-vi) were observed. In addition, membrane ruffling was apparent at 24-h incubation time point (panel vi), which is consistent with the findings regarding cytoplasmic complexity assessed by flow cytometry. These results indicate that ROFA induces an early inflammatory response, followed by increased levels of oxidant species in macrophages, possibly due to direct cell activation.

3.4. Mitochondrial function of macrophages is impaired after ROFA exposure

In order to better clarify the potential ROS sources that might explain the observed impaired redox status in ROFA-exposed macrophages, mitochondrial function was assessed, since these organelles play a relevant role in the interplay between oxidative stress and inflammation (Zhou et al., 2011). Extracellular flux analysis of oxygen consumption was performed to obtain a profile of changes in respiration rates after the addition of different mitochondria-targeted compounds (Fig. 5a). Immediately after the addition of the ATP-synthase inhibitor oligomycin, ROFA-exposed cells showed a 30% decrease ($p < 0.01$) in coupling efficiency, that is the fraction of basal respiration used for ATP synthesis, compared to the control group (Fig. 5b). Oxygen consumption rate in the presence of oligomycin provides another useful indicator of mitochondrial function, such as the proton (H^+) leak. ROFA-exposed cells exhibited a 3-fold increase in the proton leak ($p < 0.01$), which suggests mitochondrial damage that possibly leads to uncoupling (Fig. 5c). Next, the addition of the mitochondrial uncoupler FCCP generated an expected increase in oxygen consumption for the control group, which was significantly lower for ROFA-exposed cells (240 ± 40 vs. 110 ± 10% baseline OCR; $p < 0.05$). This scenario abolished spare respiratory capacity, which indicates the ability of mitochondria to respond to an increase in energy demand, in PM-exposed cells by 94% when compared to the control group ($p < 0.05$) (Fig. 5d). Another indicator of altered mitochondrial function is the loss of inner mitochondrial membrane potential. Mitochondrial membrane potential evaluated as $TMRM^+$ cells decreased by 40% ($p < 0.05$), which is closely related to the results regarding altered mitochondrial respiration (Fig. 5e and f). Nevertheless, no such alterations in mitochondrial membrane potential were observed in RAW 264.7 cells incubated with CAPs (Supplementary Fig. 3). Altogether, these results indicate that mitochondria are target organelles in the metabolic outcome that follows ROFA exposure in macrophages.

3.5. NADPH oxidase and mitochondria are relevant sources of superoxide production in ROFA-exposed macrophages

Since NADPH oxidase (NOX) is a major source of $O_2^{\bullet-}$, its activity was assessed in isolated cell membrane fractions. A 2-fold increase ($p < 0.05$) in NOX activity was observed in ROFA-exposed cells when compared to the control condition (563 ± 104 AU/min mg protein, Fig. 6a). In addition, mitochondrial $O_2^{\bullet-}$ production showed a ~2-fold increase ($p < 0.05$) in $MitoSOX^+$ cells for ROFA-exposed macrophages (Fig. 6b and c), which was not observed in CAPs-exposed cells (Supplementary Fig. 3). Taken together, these results indicate that $O_2^{\bullet-}$ produced by NOX and mitochondria could be a pivotal mediator of the observed oxidative damage following the inflammatory response triggered by ROFA incubation.

4. Discussion

Ambient air pollution exposure has been associated with increased risk of respiratory (Hamra et al., 2014) and cardiovascular diseases (Pope et al., 2019; Rajagopalan et al., 2018). The main mechanisms that lead to these adverse health effects involve the onset of local inflammation in the lung and oxidative stress (Rao et al., 2018), that might subsequently be extended into systemic circulation (Pope et al., 2016). In this scenario, alveolar macrophages play a central role in the production of inflammatory mediators and reactive oxygen species (Hussell and Bell, 2014; Marchini et al., 2016). However, there is little information regarding the sources of such mediators and whether inflammation is the initial trigger of this response. This study intends to provide evidence that links an early proinflammatory response with the occurrence of oxidative stress in macrophages, involving increased NOX activity and impaired mitochondrial function, after incubation with a PM suspension in experimental conditions that do not alter cell viability.

In order to focus on the cellular response of macrophages to PM exposure, the murine cell line RAW 264.7 was chosen. This model enabled the study of the specific response of this cell type to ambient air particles, in contrast to *in vivo* experiments where the influence of

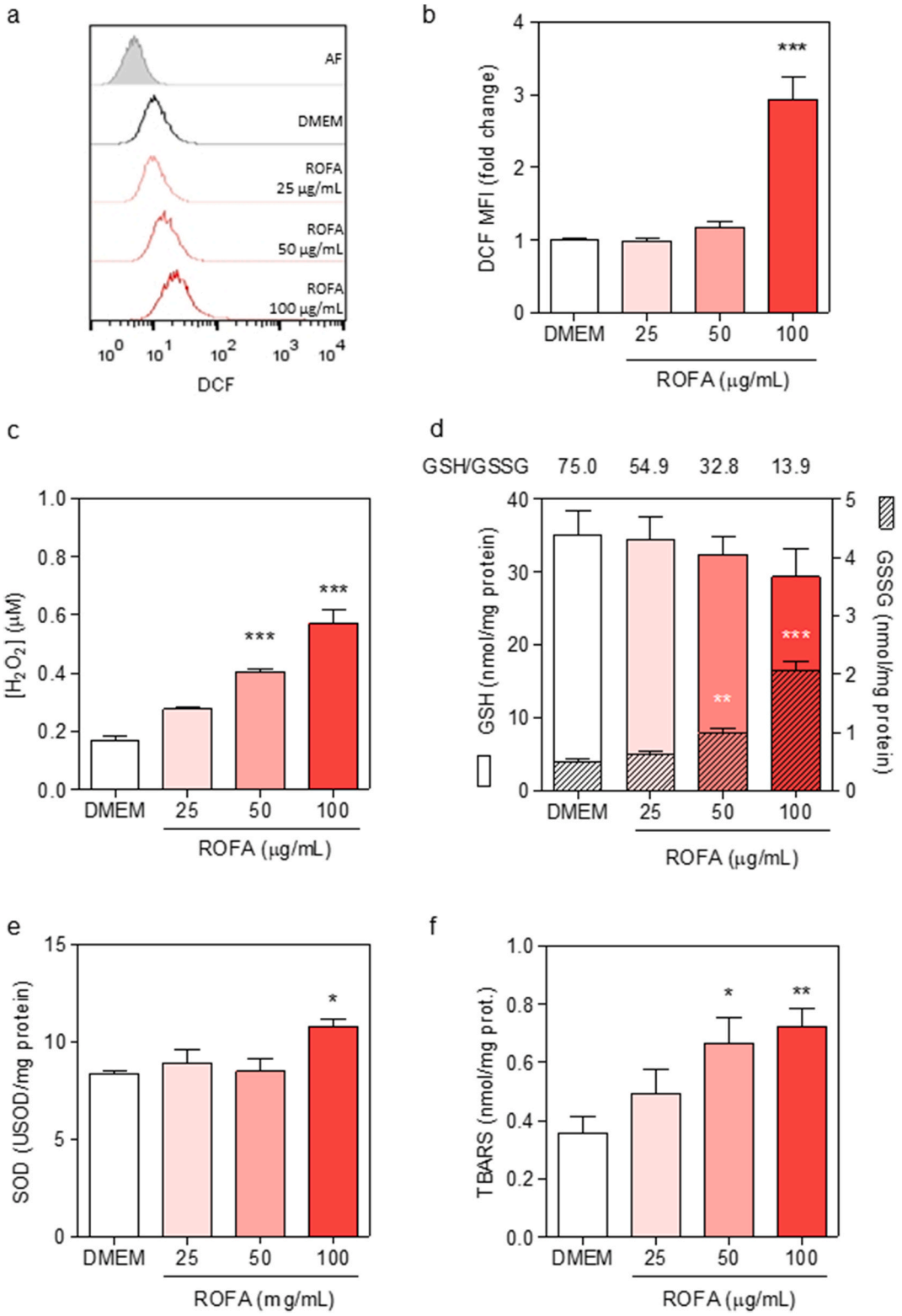

Fig. 2. Oxidative metabolism in macrophages after ROFA incubation for 24 h. Intracellular oxidant species were assessed by flow cytometry as MFI of DCF oxidation as fold change relative to DMEM group (a–b). H_2O_2 levels were quantified by the AmplexRed assay in cell culture supernatants (c). GSH and GSSG levels were measured by HPLC-MS/MS, and the GHS/GSSG ratio was obtained from the mean values (d). SOD activity was evaluated in cell lysates by the inhibition of the adrenochrome formation spectrophotometric assay (e). Oxidative damage to lipids was estimated as TBARS in whole cell lysates (f). Results are expressed as mean ± SEM of at least 3 independent experiments. *$p < 0.05$, **$p < 0.01$, ***$p < 0.001$, compared with DMEM group.

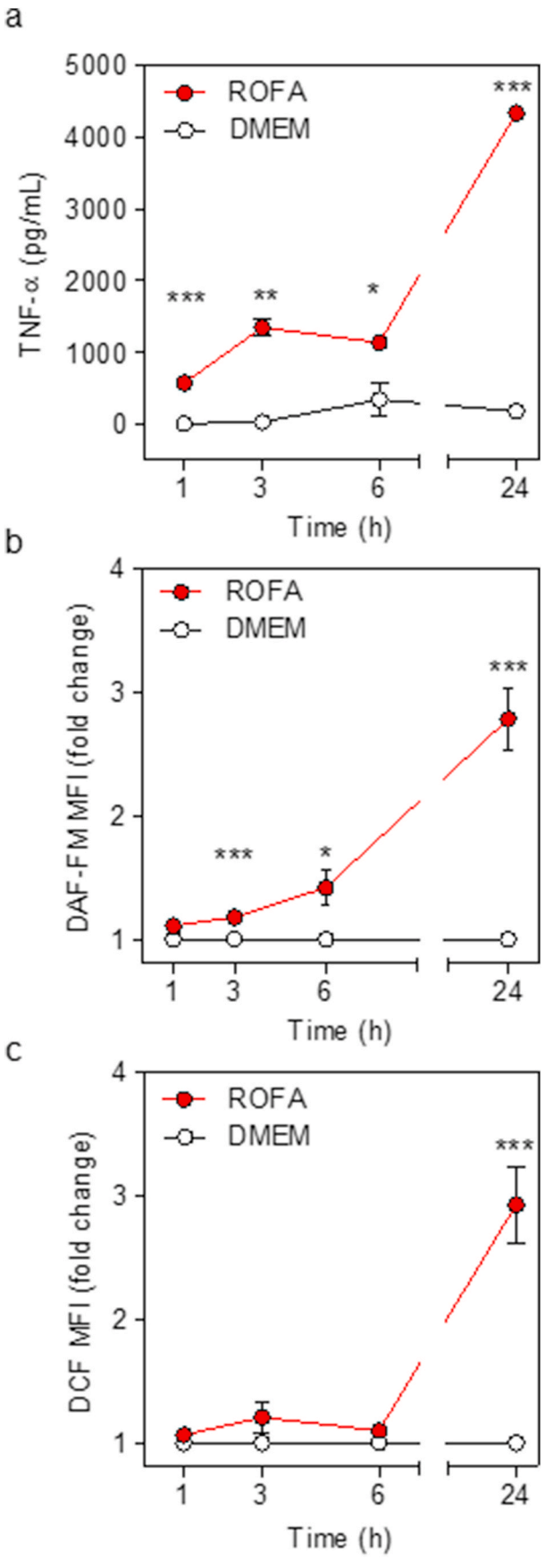

(caption on next column)

Fig. 3. Time course of inflammatory and oxidative response after incubation with ROFA 100 μg/mL. TNF-α levels were quantified by ELISA in cell culture supernatants (a). NO levels were assessed by flow cytometric analysis of fluorescent signal from the DAF-FM probe, and MFI expressed as fold change relative to the DMEM group (b). Intracellular oxidant species were assessed by flow cytometry as MFI fold change of DCF oxidation relative to the DMEM group (c). Results are expressed as mean ± SEM of at least 3 independent experiments. $^{*}p < 0.05$, $^{**}p < 0.01$, $^{***}p < 0.001$, compared with the DMEM group at the corresponding time points.

epithelial cells and other immune effectors become relevant in the development of macrophages microenvironment (Marchini et al., 2016; Musah et al., 2012). Even though oxidative stress and inflammation have been described for different PM surrogates (Steenhof et al., 2011), interesting differences emerge regarding the mechanisms linking these phenomena after exposure to PM samples of varying elemental composition (Pardo et al., 2017; Sawyer et al., 2010). Concerning the chemical nature of ROFA, its high content in metal ions made it a suitable candidate to study oxidative and inflammatory response following PM exposure. ROFA particles contain Ni and Fe in the form of soluble sulfates, which accounts for their high bioavailability and high ROFA toxicity (Pattanaik et al., 2012). Different methodological approaches have been made to test the role of metal ions absorbed in PM, such as exposure to metal-doped nanoparticles, finding a relevant contribution of Ni and Fe to the onset of oxidative alterations in the lung (Magnani et al., 2016). When such alterations lead to an imbalance between oxidants and antioxidants, in favor of the oxidants and causing a disruption of redox signaling and control and/or molecular damage, the occurrence of oxidative stress is established (Sies et al., 2017). The initial selection of the PM doses in this work is in accordance with the literature, where in order to study the mechanisms involved in the cellular response to PM, different cell types in culture were incubated with PM concentrations ranging from 25 to over 300 μg/mL (Lasagni Vitar et al., 2019; Wang et al., 2019; Xu et al., 2019). The experimental conditions in our study did not affect cell viability, indicating that the results were obtained from macrophages in an active metabolic state. Furthermore, the time course linking inflammation and oxidative stress in this model was addressed at 1, 3, 6 and 24 h of PM exposure. In this sense, our experimental approach aims to contribute to the mechanism of oxinflammation described during PM exposure.

Our results showed classical macrophage activation after PM exposure, since TNF-α and NO levels increased at early time points (1–6 h) and reached a maximum at the ultimate time point tested (24 h). These results are in accordance with a previous report showing the relevance of particle composition and size in the onset of an inflammatory response in macrophages (Jalava et al., 2008). Interestingly, DCF signal showed an increase only at the 24-h time point and the 100 μg/mL dose, revealing that an inflammatory response may precede the increase in the intracellular levels of oxidant species in this model. Since PM exposure is commonly associated with increased levels of oxidants derived from oxidases activation, for instance NOX, or redox active PM compounds, it has been proposed that damage-associated molecular patterns (DAMPs) are produced (Marchini et al., 2020). In turn, DAMPs-mediated activation of pattern recognition receptors, such as TLRs (Kampfrath et al., 2011; Shoenfelt et al., 2009), induce NF-κB pathways that lead to proinflammatory cytokines synthesis. This is the case of TNF-α, which exerts a positive feedback on reactive oxygen species generation, for instance, through the assembly of NOX2, the predominant isoform of the NADPH oxidase family found in macrophages (van der Vliet, 2011). Another proposed mechanism of the innate immune response in PM-exposed macrophages is phagocytosis. Regarding PM clearance, evidence suggests an active role of scavenger receptors, mainly represented by class A scavenger receptor (SR-A) and the macrophage receptor of collagenous structure (MARCO), by promoting the attachment and engulfment of particles (Miyata and van Eeden, 2011). A previously published report suggests that SR-A is involved in ROFA uptake

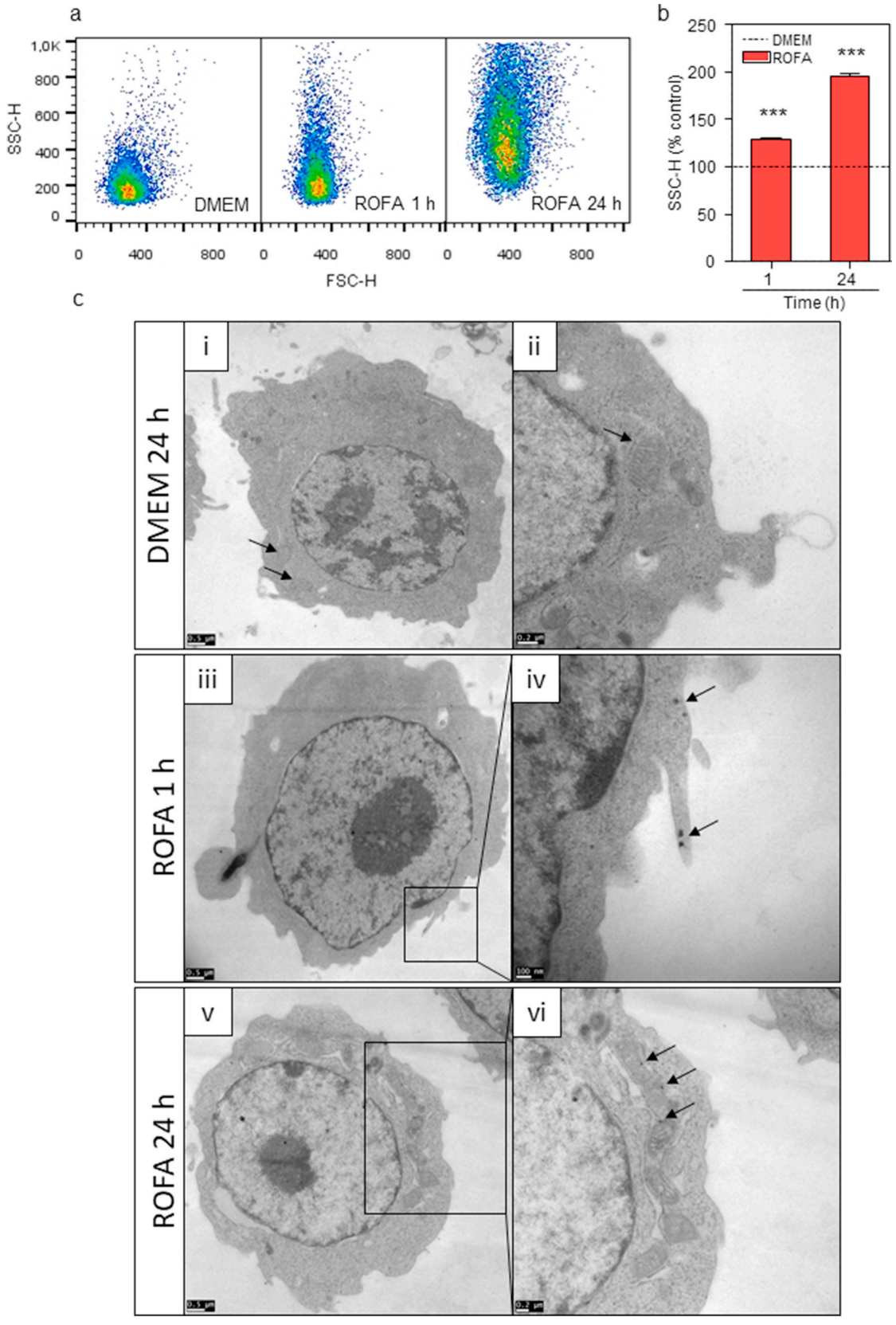

Fig. 4. Internalization of ROFA particles at 100 μg/mL exposure for 1 or 24 h. Flow cytometry assessment of light scattering properties (a) and quantification relative to the DMEM group (b). Results are expressed as mean ± SEM of at least 3 independent experiments. ***$p < 0.001$, compared with the DMEM group. Representative transmission electron microscopy imaging (c): cells in the DMEM group (i-ii) showing typical morphology and preserved mitochondria (black arrows), cells after ROFA exposure for 1 h (iii-iv) show particles in the cytoplasm and membrane protrusions (black arrows), cells after ROFA exposure for 24 h (v-vi) show mitochondrial rearrangement and particles inside the cytoplasm (black arrows). Bars: (i) 0.5 μm; (ii) 0.2 μm; (iii) 0.5 μm; (iv) 100 nm; (v) 0.5 μm; (vi) 0.2 μm.

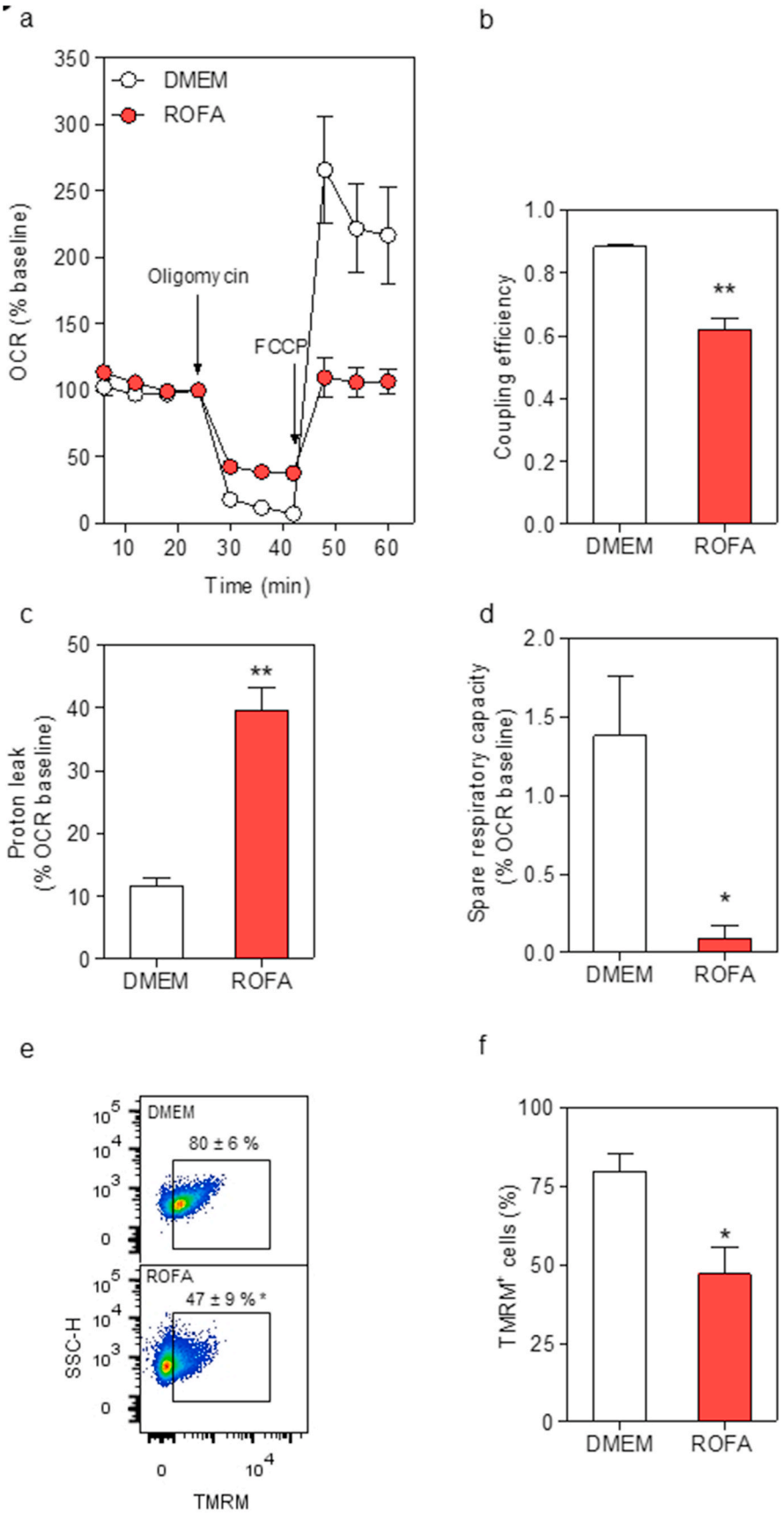

Fig. 5. Mitochondrial function of macrophages after incubation with ROFA 100 μg/mL for 24 h. Average trace of oxygen consumption rate (OCR) after the addition of the ATP synthase inhibitor oligomycin, and the uncoupler FCCP (a). Coupling efficiency was estimated as the change in basal respiration rate on addition of oligomycin (b). Spare respiratory capacity was estimated as the difference between OCR after the addition of FCCP and basal rate (c). Proton leak was estimated as the OCR in the presence of oligomycin (d). Mitochondrial membrane potential assessed by flow cytometry as $TMRM^+$ cells, as shown and quantified by the density plot (e–f). Results are expressed as mean ± SEM of at least 3 independent experiments. $^*p < 0.05$, $^{**}p < 0.01$, compared with DMEM group.

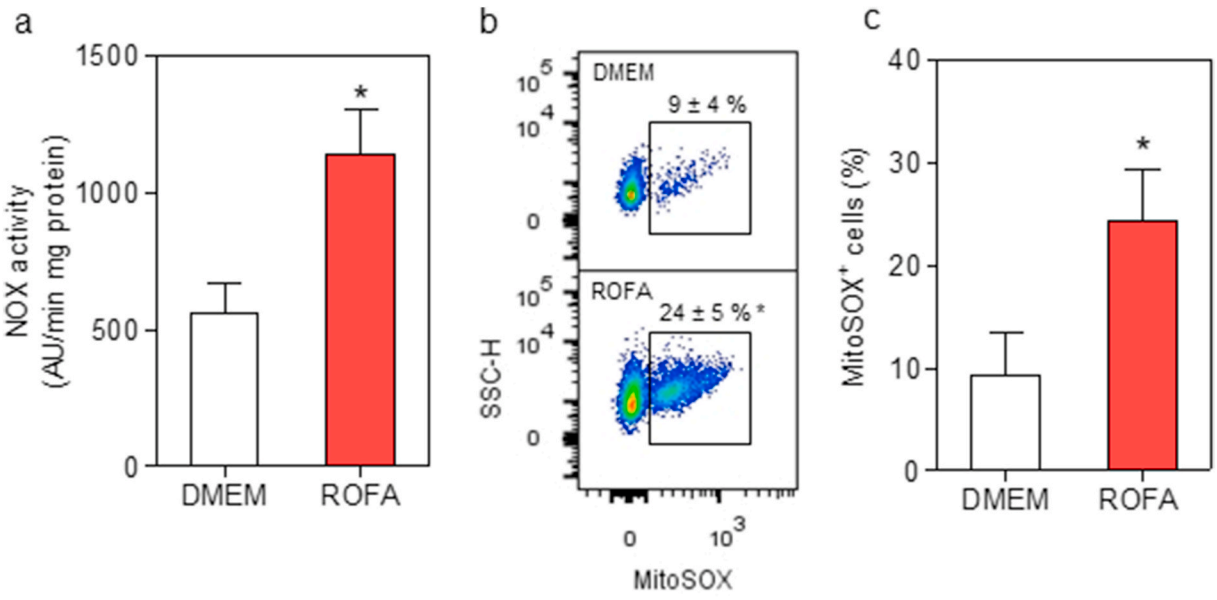

Fig. 6. $O_2^{\bullet-}$ sources in macrophages after incubation with ROFA 100 μg/mL for 24 h. NADPH oxidase (NOX) activity assessed in enriched membrane fractions by the lucigenin-derived chemiluminescence method (a). Mitochondrial $O_2^{\bullet-}$ content assessed by flow cytometry as MitoSox$^+$ cells, as shown and quantified by the density plot (b–c). Results are expressed as mean ± SEM of at least 3 independent experiments. *$p < 0.05$, compared with DMEM.

(Goldsmith et al., 1997), whereas other studies also propose the contribution of MARCO as a binding receptor for environmental particles (Arredouani et al., 2005; Thakur et al., 2008). Given the experimental protocol tested, PM uptake might be taking place, suggesting that ROFA incubation induces direct activation of macrophages, since both the early and late time points showed PM inside cell structures in transmission electron microscopy images, as previously reported in the literature (Lasagni Vitar et al., 2015; Li et al., 2003).

Based on the previously shown results, the oxidative response at the 24-h time point was thoroughly addressed. The increase in DCF signal can be attributed, at least in part, to the increase in H_2O_2 levels, for which both the mitochondria and NOX are relevant sources, as previously reported *in vivo* (Magnani et al., 2013). Changes in H_2O_2 steady state concentration has been suggested as a redox signaling mechanism that triggers protein synthesis and modulates enzyme activity (Marinho et al., 2014). This could be the case for SOD, a relevant enzyme for redox homeostasis, understood as the continuously challenged oxidative/nucleophilic balance (Ursini et al., 2016). SOD catalyzes the conversion of NOX and mitochondrial derived $O_2^{\bullet-}$ into H_2O_2, enhancing the contribution of this species in redox signaling (Brand, 2016). There is consistent evidence indicating that intracellular pro oxidative conditions might trigger the Nrf2 signaling pathway, promoting the upregulation of enzymatic and non-enzymatic antioxidant defenses (Singh et al., 2010). This model showed an altered GSH/GSSG ratio, with increased GSSG levels, consistent with the altered redox homeostasis. It may also suggest that synthesis of GSH was not affected in these experimental conditions. Consistently, SOD showed an increase in its activity, also for the highest PM dose tested. In the context of increased levels of oxidant species and onset of such antioxidant response, it is also likely to find oxidative damage to macromolecules. Accordingly, an increase in oxidative damage to lipids after PM incubation was observed, which taken together with the previously mentioned redox indicators, suggests the occurrence of oxidative stress in ROFA-exposed macrophages. In line with this evidence, a typical oxidative response has been early described for PM samples of different composition and size (Magnani et al., 2011; Michael et al., 2013).

Taking into consideration that the main alterations in oxidative metabolism took place at 24 h and ROFA 100 μg/mL incubation, and that one of the most relevant sources of reactive oxygen species are mitochondria, mitochondrial oxygen metabolism under these experimental conditions was studied. Measuring cell respiratory control is a useful general test to address mitochondrial function in intact cells (Brand and Nicholls, 2011), and in these experimental conditions it served as an indicator of an overall dysfunction in ROFA-exposed cells. The results revealed increased proton leak and poor ability to respond to an increase in energy demand, as shown by a low spare respiratory capacity. These findings were accompanied by the loss of inner membrane potential which may correspond to a lower coupling efficiency. Accordingly, previous reports have shown the influence of both soluble compounds and whole PM of diverse chemical composition in impaired mitochondrial function (Badding et al., 2014; Xia et al., 2004). Together with the reported changes in mitochondrial oxygen consumption after ROFA exposure, electron microscopy images showed a slight membrane rearrangement, predominantly at the 24 h-time point, which is supported by the shift in the SSC-H panel. This scenario may be attributable to abnormal mitochondrial morphology and membrane dynamics implicated in the inflammatory process (Gkikas et al., 2018).

The role of mitochondria in ROS generation during oxidative phosphorylation has been extensively reviewed, and most recent findings associate it with redox signaling as well as oxidative damage (Sies, 2015). In macrophages, mitochondria become key mediators of the innate immune response, as they dictate the metabolic pathway of proinflammatory cells, contribute to $O_2^{\bullet-}$/H_2O_2 production to enhance microbicidal activity, and become relevant in the initiation and restriction of the inflammasome activation (Tur et al., 2017). In the experimental model tested in this work, an increased mitochondrial production of $O_2^{\bullet-}$ in intact cells exposed to ROFA was measured, which may be a consequence of impaired mitochondrial function (Boveris and Chance, 1973). These findings suggest that mitochondria are important mediators in the events that follow PM exposure in macrophages. Interestingly, recently published evidence suggests that mitochondria are not only a source of ROS, but also a target of oxidative damage in the context of PM exposure (Valacchi et al., 2020). In this sense, the relevance of NOX2 as a source of $O_2^{\bullet-}$ in inflammatory macrophages is suggested (Griffiths et al., 2017), which encouraged the search for such contribution in this model. Indeed, an increase in NOX activity was found, which may contribute to the development of a crosstalk between the observed oxidative response and mitochondrial dysfunction. Considering these findings, it is proposed that mitochondria and NOX are the main sources of $O_2^{\bullet-}$, which is converted into H_2O_2 by SOD, and

ultimately acts as an effector molecule in redox signaling and oxidative damage to macromolecules, following PM exposure in macrophages.

5. Conclusion

Although several studies describe the impact of PM on macrophages in terms of inflammatory and oxidative response, this is the first time a comprehensive description based on the time course of PM exposure, doses, and sources of oxidant species is performed. These experimental conditions allowed the development of a possible mechanism in response to airborne PM exposure in macrophages. Inflammation leading to oxidative stress and enhanced $O_2^{\bullet-}$ production from mitochondria and NOX are the main effectors that take place in macrophages after incubation with ROFA. These findings contribute to the understanding of the mechanisms triggered in macrophages after PM exposure, which might explain the adverse health effects described in human populations, and ultimately highlights the importance of considering environmental factors in the context of respiratory and cardiovascular diseases.

Credit author statement

Lourdes Cáceres: Conceptualization, Validation, Formal analysis, Investigation, Writing - Original Draft, Writing - Review & Editing, Visualization. Mariela L. Paz: Investigation, Resources, Supervision, Writing - Review & Editing. Mariana Garcés: Investigation. Valeria Calabró: Investigation. Natalia D. Magnani: Conceptualization, Supervision. Manuela Martinefski: Investigation, Formal analysis. Pamela V. Martino Adami: Formal analysis, Writing - Review & Editing. Laura Caltana: Investigation, Formal analysis. Deborah Tasat: Resources. Laura Morelli: Resources, Writing - Review & Editing. Valeria Tripodi: Resources, Formal analysis. Giuseppe Valacchi: Resources, Writing - Review & Editing. Silvia Alvarez: Writing - Review & Editing. Daniel González Maglio: Investigation, Resources, Supervision. Timoteo Marchini: Conceptualization, Visualization, Writing - Review & Editing, Supervision. Pablo Evelson: Conceptualization, Writing - Review & Editing, Project administration, Funding acquisition.

Declaration of competing interest

The authors declare that they have no known competing financial interests or personal relationships that could have appeared to influence the work reported in this paper.

Acknowledgements

This work was supported by research grants from the University of Buenos Aires (20020170100441BA) to Dr. Pablo Evelson and from the Agencia Nacional de Promoción Científica y Tecnológica (PICT 2016–3062) to Dr. Timoteo Marchini.

The authors would like to thank Dr. Mario Contin and Dr. Romina Lasagni Vitar for their assistance in the glutathione assay and cell culture experiments, respectively, and to Dr. Diego Ojeda for technical advice on flow cytometry.

Appendix A. Supplementary data

Supplementary data to this article can be found online at https://doi.org/10.1016/j.ecoenv.2020.111186.

References

Adami, P.V.M., Quijano, C., Magnani, N., Galeano, P., Evelson, P., Cassina, A., do Carmo, S., Leal, M.C., Castaño, E.M., Cuello, A.C., Morelli, L., 2017. Synaptosomal bioenergetic defects are associated with cognitive impairment in a transgenic rat model of early Alzheimer's disease. J. Cerebr. Blood Flow Metabol. 37 (1), 69–84. https://doi.org/10.1177/0271678X15615132.

Arantes-Costa, F.M., Grund, L.Z., Martins, M.A., Lima, C., 2014. Airborne pollutant ROFA enhances the allergic airway inflammation through direct modulation of dendritic cells in an uptake-dependent mechanism. Int. Immunopharm. 22 (1), 9–20. https://doi.org/10.1016/j.intimp.2014.06.020.

Arredouani, M.S., Palecanda, A., Koziel, H., Huang, Y.-C., Imrich, A., Sulahian, T.H., Ning, Y.Y., Yang, Z., Pikkarainen, T., Sankala, M., Vargas, S.O., Takeya, M., Tryggvason, K., Kobzik, L., 2005. MARCO is the major binding receptor for unopsonized particles and bacteria on human alveolar macrophages. J. Immunol. 175 (9), 6058–6064. https://doi.org/10.4049/jimmunol.175.9.6058.

Badding, M.A., Fix, N.R., Antonini, J.M., Leonard, S.S., 2014. A comparison of cytotoxicity and oxidative stress from welding fumes generated with a new nickel-, copper-based consumable versus mild and stainless steel-based welding in RAW 264.7 mouse macrophages. PloS One 9 (6), e101310. https://doi.org/10.1371/journal.pone.0101310.

Boveris, A., Chance, B., 1973. The mitochondrial generation of hydrogen peroxide. General properties and effect of hyperbaric oxygen. Biochem. J. 134 (3), 707–716. https://doi.org/10.1042/bj1340707.

Brand, M.D., 2016. Mitochondrial generation of superoxide and hydrogen peroxide as the source of mitochondrial redox signaling. Free Radic. Biol. Med. 100, 14–31. https://doi.org/10.1016/j.freeradbiomed.2016.04.001.

Brand, M.D., Nicholls, D.G., 2011. Assessing mitochondrial dysfunction in cells. Biochem. J. 435 (2), 297–312. https://doi.org/10.1042/BJ20110162.

Breda, C.N. de S., Davanzo, G.G., Basso, P.J., Saraiva Câmara, N.O., Moraes-Vieira, P.M. M., 2019. Mitochondria as central hub of the immune system. Redox Biol 26, 101255. https://doi.org/10.1016/j.redox.2019.101255.

Brook, R.D., Rajagopalan, S., Pope, C.A., Brook, J.R., Bhatnagar, A., Diez-Roux, A.v., Holguin, F., Hong, Y., Luepker, R.v., Mittleman, M.A., Peters, A., Siscovick, D., Smith, S.C., Whitsel, L., Kaufman, J.D., 2010. Particulate matter air pollution and cardiovascular disease: an update to the scientific statement from the american heart association. Circulation 121 (21), 2331–2378. https://doi.org/10.1161/CIR.0b013e3181dbece1.

Casañas-Sánchez, V., Pérez, J.A., Quinto-Alemany, D., Díaz, M., 2016. Sub-toxic ethanol exposure modulates gene expression and enzyme activity of antioxidant systems to provide neuroprotection in hippocampal HT22 cells. Front. Physiol. 7, 312. https://doi.org/10.3389/fphys.2016.00312.

Cervellati, C., Sticozzi, C., Romani, A., Belmonte, G., de Rasmo, D., Signorile, A., Cervellati, F., Milanese, C., Mastroberardino, P.G., Pecorelli, A., Savelli, V., Forman, H.J., Hayek, J., Valacchi, G., 2015. Impaired enzymatic defensive activity, mitochondrial dysfunction and proteasome activation are involved in RTT cell oxidative damage. Biochim. Biophys. Acta 1852 (10 Pt A), 2066–2074. https://doi.org/10.1016/j.bbadis.2015.07.014.

Chen, L.C., Lippmann, M., 2009. Effects of metals within ambient air particulate matter (PM) on human health. Inhal. Toxicol. 21 (1), 1–31. https://doi.org/10.1080/08958370802105405.

Chen, Q., Vazquez, E.J., Moghaddas, S., Hoppel, C.L., Lesnefsky, E.J., 2003. Production of reactive oxygen species by mitochondria: central role of complex III. J. Biol. Chem. 278 (38), 36027–36031. https://doi.org/10.1074/jbc.M304854200.

Chen, Y., Shah, N., Huggins, F.E., Huffman, G.P., 2004. Investigation of the microcharacteristics of PM2.5 in residual oil fly ash by analytical transmission electron microscopy. Environ. Sci. Technol. 38 (24), 6553–6560. https://doi.org/10.1021/es049872h.

Gao, F., Barchowsky, A., Nemec, A.A., Fabisiak, J.P., 2004. Microbial stimulation by mycoplasma fermentans synergistically amplifies IL-6 release by human lung fibroblasts in response to residual oil fly ash (ROFA) and nickel. Toxicol. Sci. 81 (2), 467–479. https://doi.org/10.1093/toxsci/kfh205.

Ghio, A.J., Devlin, R.B., 2001. Inflammatory lung injury after bronchial instillation of air pollution particles. Am. J. Respir. Crit. Care Med. 164 (4), 704–708. https://doi.org/10.1164/ajrccm.164.4.2011089.

Ghio, A.J., Suliman, H.B., Carter, J.D., Abushamaa, A.M., Folz, R.J., 2002. Overexpression of extracellular superoxide dismutase decreases lung injury after exposure to oil fly ash. Am. J. Physiol. Lung Cell Mol. Physiol. 283 (1), L211–L218. https://doi.org/10.1152/ajplung.00409.2001.

Gkikas, I., Palikaras, K., Tavernarakis, N., 2018. The role of mitophagy in innate immunity. Front. Immunol. 9, 1283. https://doi.org/10.3389/fimmu.2018.01283.

Goldsmith, C.A., Frevert, C., Imrich, A., Sioutas, C., Kobzik, L., 1997. Alveolar macrophage interaction with air pollution particulates. Environ. Health Perspect. 105 (Suppl. 5), 1191–1195. https://doi.org/10.1289/ehp.97105s51191.

Griffiths, H.R., Gao, D., Pararasa, C., 2017. Redox regulation in metabolic programming and inflammation. Redox Biol 12, 50–57. https://doi.org/10.1016/j.redox.2017.01.023.

Hamra, G.B., Guha, N., Cohen, A., Laden, F., Raaschou-Nielsen, O., Samet, J.M., Vineis, P., Forastiere, F., Saldiva, P., Yorifuji, T., Loomis, D., 2014. Outdoor particulate matter exposure and lung cancer: a systematic review and meta-analysis. Environ. Health Perspect. 122 (9), 906–911. https://doi.org/10.1289/ehp/1408092.

Hussell, T., Bell, T.J., 2014. Alveolar macrophages: plasticity in a tissue-specific context. Nat. Rev. Immunol. 14 (2), 81–93. https://doi.org/10.1038/nri3600.

Jalava, P.I., Salonen, R.O., Pennanen, A.S., Happo, M.S., Penttinen, P., Hälinen, A.I., Sillanpää, M., Hillamo, R., Hirvonen, M.-R., 2008. Effects of solubility of urban air fine and coarse particles on cytotoxic and inflammatory responses in RAW 264.7 macrophage cell line. Toxicol. Appl. Pharmacol. 229 (2), 146–160. https://doi.org/10.1016/j.taap.2008.01.006.

Kampfrath, T., Maiseyeu, A., Ying, Z., Shah, Z., Deiuliis, J.A., Xu, X., Kherada, N., Brook, R.D., Reddy, K.M., Padture, N.P., Parthasarathy, S., Chen, L.C., Moffatt-Bruce, S., Sun, Q., Morawietz, H., Rajagopalan, S., 2011. Chronic fine particulate matter exposure induces systemic vascular dysfunction via NADPH oxidase and

TLR4 pathways. Circ. Res. 108 (6), 716–726. https://doi.org/10.1161/CIRCRESAHA.110.237560.
Lasagni Vitar, R.M., Hvozda Arana, A.G., Janezic, N.S., Marchini, T., Tau, J., Martinefski, M., Tesone, A.I., Racca, L., Reides, C.G., Tripodi, V., Evelson, P.A., Berra, A., Llesuy, S.F., Ferreira, S.M., 2019. Urban air pollution induces redox imbalance and epithelium hyperplasia in mice cornea. Toxicol. Appl. Pharmacol. 384, 114770. https://doi.org/10.1016/j.taap.2019.114770.
Lasagni Vitar, R.M., Tau, J., Reides, C.G., Berra, A., Ferreira, S.M., Llesuy, S.F., 2015. Evaluation of oxidative stress markers in human conjunctival epithelial cells exposed to diesel exhaust particles (DEP). Invest. Ophthalmol. Vis. Sci. 56 (12), 7058–7066. https://doi.org/10.1167/iovs.15-16864.
Li, N., Sioutas, C., Cho, A., Schmitz, D., Misra, C., Sempf, J., Wang, M., Oberley, T., Froines, J., Nel, A., 2003. Ultrafine particulate pollutants induce oxidative stress and mitochondrial damage. Environ. Health Perspect. 111 (4), 455–460. https://doi.org/10.1289/ehp.6000.
Liu, J., Liang, S., Du, Z., Zhang, J., Sun, B., Zhao, T., Yang, X., Shi, Y., Duan, J., Sun, Z., 2019. PM 2.5 aggravates the lipid accumulation, mitochondrial damage and apoptosis in macrophage foam cells. Environ. Pollut. 249, 482–490. https://doi.org/10.1016/j.envpol.2019.03.045.
Loffredo, L., Zicari, A.M., Occasi, F., Perri, L., Carnevale, R., Angelico, F., Del Ben, M., Martino, F., Nocella, C., De Castro, G., Cammisotto, V., Battaglia, S., Duse, M., Violi, F., 2018a. Role of NADPH oxidase-2 and oxidative stress in children exposed to passive smoking. Thorax 73 (10), 986–988. https://doi.org/10.1136/thoraxjnl-2017-211293.
Loffredo, L., Zicari, A.M., Occasi, F., Perri, L., Carnevale, R., Battaglia, S., Angelico, F., Del Ben, M., Martino, F., Nocella, C., Farcomeni, A., De Castro, G., Duse, M., Violi, F., 2018b. Passive smoking exacerbates nicotinamide-adenine dinucleotide phosphate oxidase isoform 2–induced oxidative stress and arterial dysfunction in children with persistent allergic rhinitis. J. Pediatr. 202, 252–257. https://doi.org/10.1016/j.jpeds.2018.06.053.
Magnani, N.D., Marchini, T., Garcés, M., Mebert, A., Cáceres, L., Diaz, L., Desimone, M., Evelson, P.A., 2016. Role of transition metals present in air particulate matter on lung oxygen metabolism. Int. J. Biochem. Cell Biol. 81 (Pt B), 419–426. https://doi.org/10.1016/j.biocel.2016.10.009.
Magnani, N.D., Marchini, T., Tasat, D.R., Alvarez, S., Evelson, P.A., 2011. Lung oxidative metabolism after exposure to ambient particles. Biochem. Biophys. Res. Commun. 412 (4), 667–672. https://doi.org/10.1016/j.bbrc.2011.08.021.
Magnani, N.D., Marchini, T., Vanasco, V., Tasat, D.R., Alvarez, S., Evelson, P., 2013. Reactive oxygen species produced by NADPH oxidase and mitochondrial dysfunction in lung after an acute exposure to Residual Oil Fly Ashes. Toxicol. Appl. Pharmacol. 270 (1), 31–38. https://doi.org/10.1016/j.taap.2013.04.002.
Magnani, N.D., Muresan, X.M., Belmonte, G., Cervellati, F., Sticozzi, C., Pecorelli, A., Miracco, C., Marchini, T., Evelson, P., Valacchi, G., 2015. Skin damage mechanisms related to airborne particulate matter exposure. Toxicol. Sci. 149 (1), 227–236. https://doi.org/10.1093/toxsci/kfv230.
Marchini, T., D'Annunzio, V., Paz, M.L., Cáceres, L., Garcés, M., Perez, V., Tasat, D., Vanasco, V., Magnani, N., Gonzalez Maglio, D., Gelpi, R.J., Alvarez, S., Evelson, P., 2015. Selective TNF-α targeting with infliximab attenuates impaired oxygen metabolism and contractile function induced by an acute exposure to air particulate matter. Am. J. Physiol. Heart Circ. Physiol. 309 (10), H1621–H1628. https://doi.org/10.1152/ajpheart.00359.2015.
Marchini, T., Magnani, N.D., Paz, M.L., Vanasco, V., Tasat, D., González Maglio, D.H., Alvarez, S., Evelson, P.A., 2014. Time course of systemic oxidative stress and inflammatory response induced by an acute exposure to Residual Oil Fly Ash. Toxicol. Appl. Pharmacol. 274 (2), 274–282. https://doi.org/10.1016/j.taap.2013.11.013.
Marchini, T., Wolf, D., Michel, N.A., Mauler, M., Dufner, B., Hoppe, N., Beckert, J., Jäckel, M., Magnani, N., Duerschmied, D., Tasat, D., Alvarez, S., Reinöhl, J., von zur Muhlen, C., Idzko, M., Bode, C., Hilgendorf, I., Evelson, P., Zirlik, A., 2016. Acute exposure to air pollution particulate matter aggravates experimental myocardial infarction in mice by potentiating cytokine secretion from lung macrophages. Basic Res. Cardiol. 111 (4), 44. https://doi.org/10.1007/s00395-016-0562-5.
Marchini, T., Zirlik, A., Wolf, D., 2020. Pathogenic role of air pollution particulate matter in cardiometabolic disease: evidence from mice and humans. Antioxidants Redox Signal. 33 (4), 263–279. https://doi.org/10.1089/ars.2020.8096.
Marinho, H.S., Real, C., Cyrne, L., Soares, H., Antunes, F., 2014. Hydrogen peroxide sensing, signaling and regulation of transcription factors. Redox Biol 2, 535–562. https://doi.org/10.1016/j.redox.2014.02.006.
Martin, P.J., Héliot, A., Trémolet, G., Landkocz, Y., Dewaele, D., Cazier, F., Ledoux, F., Courcot, D., 2019. Cellular response and extracellular vesicles characterization of human macrophages exposed to fine atmospheric particulate matter. Environ. Pollut. 254 (Pt A), 112933. https://doi.org/10.1016/j.envpol.2019.07.101.
Michael, S., Montag, M., Dott, W., 2013. Pro-inflammatory effects and oxidative stress in lung macrophages and epithelial cells induced by ambient particulate matter. Environ. Pollut. 183, 19–29. https://doi.org/10.1016/j.envpol.2013.01.026.
Miyata, R., van Eeden, S.F., 2011. The innate and adaptive immune response induced by alveolar macrophages exposed to ambient particulate matter. Toxicol. Appl. Pharmacol. 257 (2), 209–226. https://doi.org/10.1016/j.taap.2011.09.007.
Moon, J.H., Kim, T.H., Lee, H.M., Lee, Hoon, Seung, Choe, W., Kim, H.K., Lee, J.H., Oh, K.H., Lee, Sang Hag, 2009. Overexpression of the superoxide anion and NADPH oxidase isoforms1 and 4 (NOX1 and NOX4) in allergic nasal mucosa. Am. J. Rhinol. Allergy. 23 (4), 370–376. https://doi.org/10.2500/ajra.2009.23.3340.
Musah, S., DeJarnett, N., Hoyle, G.W., 2012. Tumor necrosis factor-α mediates interactions between macrophages and epithelial cells underlying proinflammatory gene expression induced by particulate matter. Toxicology 299 (2–3), 125–132. https://doi.org/10.1016/j.tox.2012.05.014.
Orona, N.S., Astort, F., Maglione, G.A., Saldiva, P.H.N., Yakisich, J.S., Tasat, D.R., 2014. Direct and indirect air particle cytotoxicity in human alveolar epithelial cells. Toxicol. Vitro 28 (5), 796–802. https://doi.org/10.1016/j.tiv.2014.02.011.
Pardo, M., Katra, I., Schaeur, J.J., Rudich, Y., 2017. Mitochondria-mediated oxidative stress induced by desert dust in rat alveolar macrophages. Geohealth 1 (1), 4–16. https://doi.org/10.1002/2016GH000017.
Pattanaik, S., Huggins, F.E., Huffman, G.P., 2012. Chemical speciation of Fe and Ni in residual oil fly ash fine particulate matter using X-ray absorption spectroscopy. Environ. Sci. Technol. 46 (23), 12927–12935. https://doi.org/10.1021/es301080s.
Pope, C.A., Bhatnagar, A., McCracken, J.P., Abplanalp, W., Conklin, D.J., O'Toole, T., 2016. Exposure to fine particulate air pollution is associated with endothelial injury and systemic inflammation. Circ. Res. 119 (11), 1204–1214. https://doi.org/10.1161/CIRCRESAHA.116.309279.
Pope, C.A., Lefler, J.S., Ezzati, M., Higbee, J.D., Marshall, J.D., Kim, S.Y., Bechle, M., Gilliat, K.S., Vernon, S.E., Robinson, A.L., Burnett, R.T., 2019. Mortality risk and fine particulate air pollution in a large, representative cohort of U.S. Adults. Environ. Health Perspect. 127 (7), 77007. https://doi.org/10.1289/EHP4438.
Prado, C.M., Righetti, R.F., Lopes, F D T Q D S, Leick, E.A., Arantes-Costa, F.M., de Almeida, F.M., Saldiva, P.H.N., Mauad, T., Tibério, I.D.F.L.C., Martins, M.D.A., 2019. INOS inhibition reduces lung mechanical alterations and remodeling induced by particulate matter in mice. Pulm. Med. 2019, 4781528. https://doi.org/10.1155/2019/4781528.
Rajagopalan, S., Al-Kindi, S.G., Brook, R.D., 2018. Air pollution and cardiovascular disease: JACC state-of-the-art review. J. Am. Coll. Cardiol. 72 (17), 2054–2070. https://doi.org/10.1016/j.jacc.2018.07.099.
Rao, X., Zhong, J., Brook, R.D., Rajagopalan, S., 2018. Effect of particulate matter air pollution on cardiovascular oxidative stress pathways. Antioxidants Redox Signal. 28 (9), 797–818. https://doi.org/10.1089/ars.2017.7394.
Sawyer, K., Mundandhara, S., Ghio, A.J., Madden, M.C., 2010. The effects of ambient particulate matter on human alveolar macrophage oxidative and inflammatory responses. J. Toxicol. Environ. Health A. 73 (1), 41–57. https://doi.org/10.1080/15287390903248901.
Shoenfelt, J., Mitkus, R.J., Zeisler, R., Spatz, R.O., Powell, J., Fenton, M.J., Squibb, K.A., Medvedev, A.E., 2009. Involvement of TLR2 and TLR4 in inflammatory immune responses induced by fine and coarse ambient air particulate matter. J. Leukoc. Biol. 86 (2), 303–312. https://doi.org/10.1189/jlb.1008587.
Sies, H., 2015. Oxidative stress: a concept in redox biology and medicine. Redox Biol 4, 180–183. https://doi.org/10.1016/j.redox.2015.01.002.
Sies, H., Berndt, C., Jones, D.P., 2017. Oxidative stress: annual review of biochemistry. Annu. Rev. Biochem. 86, 715–748. https://doi.org/10.1146/annurev-biochem-061516-045037.
Sijan, Z., Antkiewicz, D.S., Heo, J., Kado, N.Y., Schauer, J.J., Sioutas, C., Shafer, M.M., 2015. An in Vitro alveolar macrophage assay for the assessment of inflammatory cytokine expression induced by atmospheric particulate matter. Environ. Toxicol. 30 (7), 836–851. https://doi.org/10.1002/tox.21961.
Singh, S., Vrishni, S., Singh, B.K., Rahman, I., Kakkar, P., 2010. Nrf2-ARE stress response mechanism: a control point in oxidative stress-mediated dysfunctions and chronic inflammatory diseases. Free Radic. Res. 44 (11), 1267–1288. https://doi.org/10.3109/10715762.2010.507670.
Steenhof, M., Gosens, I., Strak, M., Godri, K.J., Hoek, G., Cassee, F.R., Mudway, I.S., Kelly, F.J., Harrison, R.M., Lebret, E., Brunekreef, B., Janssen, N.A.H., Pieters, R.H.H., 2011. In vitro toxicity of particulate matter (PM) collected at different sites in The Netherlands is associated with PM composition, size fraction and oxidative potential–the RAPTES project. Part. Fibre Toxicol 8, 26. https://doi.org/10.1186/1743-8977-8-26.
Tang, Q., Huang, K., Liu, J., Wu, S., Shen, D., Dai, P., Li, C., 2019. Fine particulate matter from pig house induced immune response by activating TLR4/MAPK/NF-KB pathway and NLRP3 inflammasome in alveolar macrophages. Chemosphere 236, 124373. https://doi.org/10.1016/j.chemosphere.2019.124373.
Thakur, S.A., Hamilton, R.F., Holian, A., 2008. Role of scavenger receptor A family in lung inflammation from exposure to environmental particles. J. Immunot. 5 (2), 151–157. https://doi.org/10.1080/15476910802085863.
Tur, J., Vico, T., Lloberas, J., Zorzano, A., Celada, A., 2017. Macrophages and mitochondria: a critical interplay between metabolism, signaling, and the functional activity. Adv. Immunol. 133, 1–36. https://doi.org/10.1016/bs.ai.2016.12.001.
Ursini, F., Maiorino, M., Forman, H.J., 2016. Redox homeostasis: the Golden Mean of healthy living. Redox Biol 8, 205–215. https://doi.org/10.1016/j.redox.2016.01.010.
Valacchi, G., Cervellati, C., Evelson, P., Rahman, I., 2016. Redox regulation of inflammatory processes. Int. J. Biochem. Cell Biol. 81 (Pt B), 234–235. https://doi.org/10.1016/j.biocel.2016.11.002.
Valacchi, G., Magnani, N., Woodby, B., Ferreira, S.M., Evelson, P., 2020. Particulate matter induces tissue OxInflammation: from mechanism to damage. Antioxidants Redox Signal. 33 (4), 308–326. https://doi.org/10.1089/ars.2019.8015.
Valacchi, G., Virgili, F., Cervellati, C., Pecorelli, A., 2018. OxInflammation: from subclinical condition to pathological biomarker. Front. Physiol. 9, 858. https://doi.org/10.3389/fphys.2018.00858.
van der Vliet, A., 2011. NOX enzymes in allergic airway inflammation. Biochim. Biophys. Acta 1810 (11), 1035–1044. https://doi.org/10.1016/j.bbagen.2011.03.004.
Wang, G., Zhang, X., Liu, X., Zheng, J., Chen, R., Kan, H., 2019. Ambient fine particulate matter induce toxicity in lung epithelial-endothelial co-culture models. Toxicol. Lett. 301, 133–145. https://doi.org/10.1016/j.toxlet.2018.11.010.
WHO, 2018. Burden of disease from the joint effects of household and ambient Air pollution for 2016. WHO report. Available at: https://www.who.int/airpollution/data/AP_joint_effect_BoD_results_May2018.pdf. .

Xia, T., Korge, P., Weiss, J.N., Li, N., Venkatesen, M.I., Sioutas, C., Nel, A., 2004. Quinones and aromatic chemical compounds in particulate matter induce mitochondrial dysfunction: implications for ultrafine particle toxicity. Environ. Health Perspect. 112 (14), 1347–1358. https://doi.org/10.1289/ehp.7167.

Xu, Z., Li, Z., Liao, Z., Gao, S., Hua, L., Ye, X., Wang, Y., Jiang, S., Wang, N., Zhou, D., Deng, X., 2019. PM 2.5 induced pulmonary fibrosis in vivo and in vitro. Ecotoxicol. Environ. Saf. 171, 112–121. https://doi.org/10.1016/j.ecoenv.2018.12.061.

Zhao, Q., Chen, H., Yang, T., Rui, W., Liu, F., Zhang, F., Zhao, Y., Ding, W., 2016. Direct effects of airborne PM2.5 exposure on macrophage polarizations. Biochim. Biophys. Acta 1860 (12), 2835–2843. https://doi.org/10.1016/j.bbagen.2016.03.033.

Zhou, R., Yazdi, A.S., Menu, P., Tschopp, J., 2011. A role for mitochondria in NLRP3 inflammasome activation. Nature 469 (7329), 221–225. https://doi.org/10.1038/nature09663.